CrossMark

RESEARCH PAPER

Allowable stresses in high-frequency mechanical impact (HFMI)-treated joints subjected to variable amplitude loading

Eeva Mikkola[1,2] · Heikki Remes[1]

Abstract The effectiveness of high-frequency mechanical impact (HFMI) is considered to rely on the existence of compressive residual stresses. To determine when residual stress relaxation occurs, and what the resulting influence on fatigue improvement is, local stress-strain response in as-welded and HFMI-treated weld toes was modelled under different peak stress conditions. Then, effective notch stress analysis was used to correlate these results with available experimental observations. The simulations showed that high stress ratios and compressive peak stresses were critical with respect to residual stress relaxation, as expected. A compressive peak stress of $0.6f_y$ (nominal yield strength) resulted in full residual stress relaxation. The relative fatigue damage calculations and the notch stress analysis indicated, however, that fatigue improvement could be expected even after significant residual stress relaxation. Based on this and previously observed benefit for high stress ratios, an increase in maximum allowable stresses for HFMI-treated welded steel joints is suggested. The maximum stress ratio is proposed to be increased from $R = 0.52$ to $R = 0.7$, and the maximum stress range to limit compressive stresses is proposed to be increased from $\Delta S_{max} = 0.9f_y$ to $\Delta S_{max} = 1.2f_y$, which corresponds to $S_{min} = -0.6f_y$ for stress ratio $R = -1$.

Recommended for publication by Commission XIII - Fatigue of Welded Components and Structures

✉ Eeva Mikkola
   eeva.mikkola@vtt.fi

1   Department of Mechanical Engineering, Aalto University,
    P.O. Box 14300, FI-00076 Aalto, Finland

2   Technical Research Centre of Finland, P.O. Box 1000, FI-02044
    VTT Espoo, Finland

Nomenclature

D	Damage sum
FAT	Characteristic fatigue class in MPa corresponding to 2×10^6 cycles at failure with a survival probability of 95 % based on two-sided confidence limits at a confidence level of 75 % (discrete value)
f_y	Yield strength
k	Number of data points
K_n	Notch stress factor
m/m'	S–N curve (inverse) slope below/above the knee point
N	Number of cycles
P_{SWT}	Smith-Watson-Topper parameter
r	Notch or weld toe radius
R	Stress ratio (S_{min}/S_{max})
S	Nominal stress
t	Plate thickness
ε	Strain
σ	Stress

Subscripts and modifiers

c	Characteristic value
eq	Equivalent value
i/j	Value below/above S–N curve knee point
max/min	Maximum/minimum value
n	Notch value
Δ	Range

1 Introduction

High-frequency mechanical impact (HFMI) is an effective and user-friendly means for improving the fatigue strength of welded steel joints. In addition, the method provides potential for lightweight design, as the fatigue strength of HFMI-treated joints increases with increasing steel strength [1, 2]. The obtained improvement is mainly attributed to compressive residual stresses induced at the weld toe, but the treatment also improves the weld toe geometry and strain hardens the treated region. Due to an increasing interest in the method, a fatigue assessment guidelines proposal for HFMI-treated joints was published in 2013 [3]. The proposal was mainly based on experimental evidence from small-scale specimens subjected to constant amplitude (CA) loading with a stress ratio of $R = 0.1$. Under typical service loading, however, both the stress range and mean stress fluctuate from one cycle to the next.

In general, the benefit from different peening and mechanical impact treatments is considered to rely on the existence of compressive residual stresses. These can relax due to high stress ratios and peak stresses during service loading, when local stress exceeds local yield strength [4]. Therefore, the current International Institute of Welding (IIW) recommendations on fatigue improvement [5] limit allowable stresses in hammer and needle peened joints. The maximum allowable stress is $0.8f_y$, where f_y is the yield strength, and the maximum allowable stress ratio is $R = 0.5$. Following this, allowable stress ratio and maximum stresses were limited in the fatigue assessment guidelines proposed for HFMI-treated joints [3]. In the proposal, benefit from HFMI must be confirmed experimentally if the maximum nominal stress range exceeds $0.8f_y(1-R)$ or $0.9f_y$, where f_y is the nominal yield strength, or the applied stress ratio exceeds $R = 0.52$. $0.9f_y$ is meant to limit large compressive peak stresses.

To determine the applicability of the allowable stress ratio and stress range limits proposed in [3], fatigue data on high stress ratio and variable amplitude (VA) loading were analysed statistically by Mikkola et al. [6, 7]. The data were compared to the proposed characteristic curves [3] using nominal stress method as described in Mikkola et al. [6]. Three joint types were investigated: double-sided non-load-carrying transverse attachments, double-sided longitudinal attachments and butt joints. The plate thickness ranged from 5 to 30 mm, and the yield strengths ranged from 355 to 960 MPa. In total, 265 data points were analysed, of which 49 were subjected to VA loading and 216 were subjected to CA loading under stress ratios $0.17 < R \leq 0.75$.

Comparison of the CA data [8–14] and the proposed characteristic curves for HFMI [3] showed that most of the data points fell clearly above the proposed HFMI curves. The calculated characteristic fatigue strengths at 2×10^6 cycles were close to or clearly higher than the assumed fatigue classes. In addition, the analysis showed that improvement with respect to as-welded (AW) state could remain for stress ratios up to $R = 0.7$. Some of the CA test conditions exceeded the maximum allowable stress range of $\Delta S_{max} = 0.8f_y(1-R)$. Despite this, the data fitted the proposed curves: only one of these data points fell below the HFMI curve. However, the benefit from HFMI treatment clearly decreased with increasing stress range until no improvement was observed, as suggested by the proposed maximum stress range limit. Comparison of the VA data [10, 15–17] with the proposed characteristic curves for HFMI [3] showed that all data points fell above the proposed HFMI curves even though most of the test conditions exceeded the $\Delta S_{max} = 0.9f_y$ limit for negative stress ratios. The maximum stress range was considered to correspond to the largest individual cycle in the spectrum.

Based on the available CA data, it was stated that the given stress ratio and maximum stress range limits could be used to describe the effect of high stress ratios on fatigue improvement in HFMI-treated welded joints. However, the allowable maximum stress ratio was suggested to be increased from $R = 0.52$ to $R = 0.7$ [7]. The VA loading data analysis indicated, however, that the proposed allowable stress limit of $\Delta S_{max} = 0.9f_y$ was overly conservative for $R = -1$ VA loading. This was attributed to uncertainty in residual stress relaxation behaviour and possible benefit from geometry improvement and strain hardening at the weld toe. Therefore, a better understanding of when residual stress relaxation occurs and what is the resulting impact on fatigue strength improvement is needed to build a solid basis for fatigue assessment guidelines for HFMI-treated joints.

The aim of this work is to determine allowable stress limits for HFMI-treated welded steel joints. It is known that residual stress relaxation depends on the relationship of local stress and local yield behaviour. Therefore, residual stress relaxation and the resulting fatigue damage were studied in Mikkola et al. [18]. Results of this work are discussed and used here to estimate residual stress relaxation and its influence on fatigue improvement under VA loading. Peak stresses in the simulations and available experimental VA loading data are correlated using effective notch stress analysis, as described in Mikkola [19]. Finally, based on the presented analyses and existing proposal for HFMI-treated joints [3], an increase in allowable stress limits for HFMI-treated joints is suggested. The existing proposal is shortly described in Sect. 2.

2 Existing fatigue assessment proposal for HFMI-treated joints

The proposed fatigue assessment guidelines for HFMI-treated welded steel joints [3] apply to plate thicknesses of 5 to 50 mm and steels with nominal yield strengths of 235 MPa $\leq f_y \leq$ 960 MPa. The proposal considers fatigue assessment based on nominal stress, structural hot spot stress, and

effective notch stress. Here, the focus is on the effective notch stress method, as it is used in the subsequent analysis. Figure 1 illustrates the proposed improvement in terms of effective notch stress assuming a reference radius of 1 mm. For AW joints, the S–N curve slope is $m = 3$, and the fatigue class is fixed at FAT 225 for all joint types. In the IIW system, FAT is determined as the fatigue strength at 2×10^6 cycles with 95 % survival probability, where the survival probability is based on two-sided confidence limits at a confidence level of 75 % [20]. For HFMI-improved joints, the S–N curve slope is $m = 5$. Below the knee point, which in the IIW system [20] is defined as 10^7 cycles, the S–N curve slopes for AW and HFMI-treated joints are $m' = 22$ for CA loading and $m' = 2 m-1$ for VA loading. For steels with specified yield strengths $f_y \le 355$ MPa, the proposed fatigue strength improvement due to HFMI corresponds to an increase of four fatigue classes from AW state. For specified yield strengths $f_y > 355$ MPa, the number of fatigue classes increases by one for every 200 MPa increase in yield strength. Maximum improvement is eight fatigue classes. Note that for very high stress ranges, the characteristic curves for HFMI can be below the AW curve. It is assumed, however, that AW curve gives the minimum fatigue life, as it is considered highly improbable that HFMI treatment would deteriorate the joint. Finally, the highest S–N curve that can be claimed following HFMI improvement is FAT 180. This is one fatigue class greater than the IIW curve for machined plate edges. Marquis et al. [3] have proposed this based on several studies.

CA and VA loading are correlated using equivalent stress range [21]:

$$\Delta S_{eq} = \left(\frac{1}{D} \cdot \frac{\sum \Delta S_i^m N_i + \Delta S_k^{(m-m')} \cdot \sum \Delta S_j^{m'} N_j}{\sum N_i + \sum N_j} \right)^{\frac{1}{m}}. \quad (1)$$

Table 1 Minimum reduction in the number of FAT classes with respect to fatigue strength improvement for HFMI-treated welded joints based on R ratio [3]

R-ratio	Minimum FAT class reduction
$R \le 0.15$	No reduction due to stress ratio
$0.15 < R \le 0.28$	Reduction by one FAT class
$0.28 < R \le 0.4$	Reduction by two FAT classes
$0.4 < R \le 0.52$	Reduction by three FAT classes
$R > 0.52$	No data available. The degree of improvement must be confirmed by testing.

In Eq. (2), ΔS_k is the stress range associated with the knee point in the S–N curve, ΔS_i and N_i are the stress range and number of cycles for cycles with stresses higher than the knee point stress, and ΔS_j and N_j are the stress range and number of cycles for cycles with stresses lower than the knee point stress. D is the damage sum, e.g. 0.5 or 1.0 [20], and m and m' are the above and below knee point S–N curve slopes. To prevent residual stress relaxation, applied stress ratio and maximum nominal stresses are limited. The influence of increasingly positive stress ratios $R > 0.15$ is expressed as penalties with respect to fatigue strength improvement according to Table 1 [3]. The maximum allowable stress in loading history is $S_{max} > 0.8f_y$. In addition, to limit large compressive reversals, maximum allowable stress range is limited to $\Delta S \le 0.9f_y$. In terms of the maximum nominal stress range, the limits are

$$\begin{cases} \Delta S_{max} \le 0.8 f_y (1-R), \text{ for} -0.125 \le R \le 0.52 \\ \Delta S_{max} \quad \le 0.9 f_y, \text{ for} -1 \le R < -0.125 \end{cases}. \quad (2)$$

For nominal stresses above these limits, benefit from HFMI treatment cannot be claimed without testing.

Fig. 1 Characteristic effective notch stress S–N curves for HFMI-improved and AW joints when $R \le 0.15$ under CA loading for various steel grades as proposed in Marquis et al. [3]
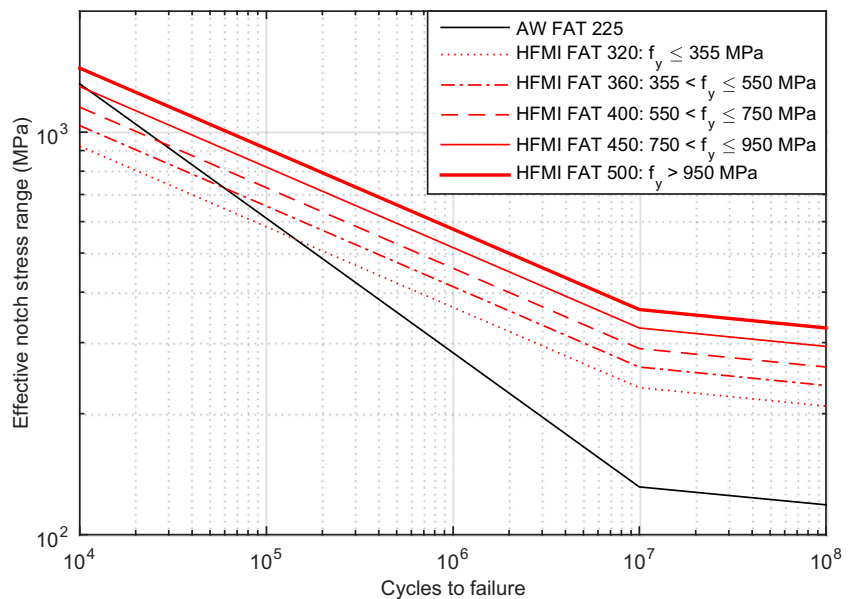

Legend:
— AW FAT 225
··· HFMI FAT 320: $f_y \le 355$ MPa
-·- HFMI FAT 360: $355 < f_y \le 550$ MPa
-- HFMI FAT 400: $550 < f_y \le 750$ MPa
— HFMI FAT 450: $750 < f_y \le 950$ MPa
— HFMI FAT 500: $f_y > 950$ MPa

Axis labels: Effective notch stress range (MPa) vs Cycles to failure

Table 2 Simulated joint conditions with properties at weld toe, i.e. the assumed crack initiation location with RS corresponding to residual stress and HAZ corresponding to heat-affected zone [18]

	Residual stresses	Notch geometry	Material condition
1) AW	Tensile	AW	HAZ
2) RS (HFMI)	Compressive	AW	HAZ
3) RS + Geometry (HFMI)	Compressive	HFMI-groove	HAZ
4) Full HFMI	Compressive	HFMI-groove	HFMI

1) → 2) Residual stress effect

2) → 3) Geometry effect

3) → 4) Strain hardening effect

3 Numerical analyses of HFMI-treated joints

3.1 Elastic-plastic analysis of HFMI-treated transverse attachment

The influence of different stress ratios and peak stresses on residual stress relaxation and fatigue damage was simulated in a previous study by Mikkola et al. [18]. A transverse non-load-carrying joint with double-sided attachments subjected to axial loading was modelled with 2D finite elements (FE) in different conditions, as described in Table 2, with FE program Abaqus [22]. AW represented AW weld toe condition with tensile residual stresses, unimproved notch geometry and heat-affected zone (HAZ) material condition at the fatigue critical weld toe. To separate the residual stress, geometry and strain hardening effects, HFMI condition was modelled in three stages:

1. RS (HFMI) with only compressive residual stresses at the weld toe
2. RS + geometry (HFMI) with compressive residual stresses and geometry improvement at the weld toe
3. Full HFMI with compressive residual stresses, geometry improvement and strain hardened material condition at the weld toe

Figure 2 shows how the different material property and residual stress regions were applied. The residual stress distributions applied to the indicated RS regions were based on X-ray residual stress measurements on AW and HFMI-treated S700 joints by Yıldırım and Marquis [16] and Suominen et al. [24]. The residual stress distributions were introduced to Abaqus as temperature fields according to the coordinate system shown in Fig. 2. The input and modelled residual stress distributions for the different joint conditions are shown in Fig. 3. Close to y = 0, the input and modelled distributions differ depending on local geometry and material condition because of localized plasticity at the weld toe. However, the only result of these differences in near surface values is that the geometry effect (see Table 2) could be underestimated in the subsequent simulations.

As shown by Fig. 2, the HAZ and HFMI region thicknesses were both 1 mm. Base material properties were assumed for weld metal region. Combined nonlinear isotropic-kinematic hardening [22] was used to describe the elastic-plastic material behaviour. Elastic response was determined by elastic modulus 210 GPa and Poisson's ratio of 0.3. Measured cyclic stress–strain response at half-life for S700 BM, HAZ and HFMI-1 conditions from Mikkola et al. [15] were fitted to the combined nonlinear isotropic-kinematic hardening model. As most of the cyclic softening took place before half-life, cyclic softening after half-life was not taken into account. A comparison of
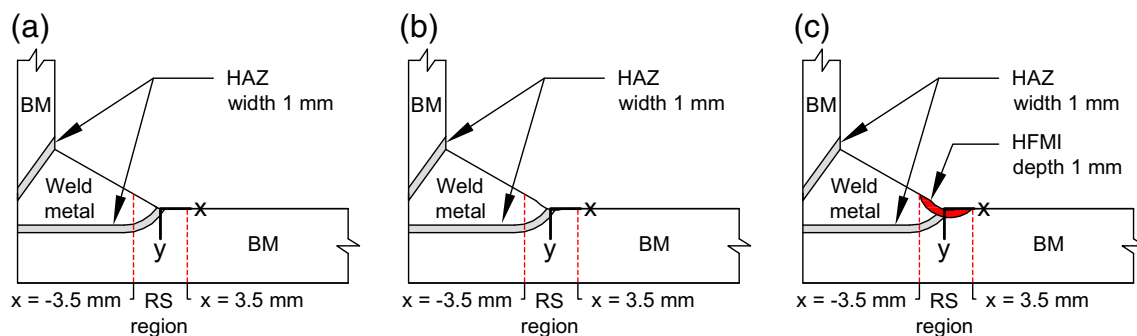
Fig. 2 Schematic view of modelled configurations **a** AW and RS (HFMI), **b** RS + geometry (HFMI) and **c** full HFMI [18], where RS indicates region, where initial residual stress state was nonzero and BM signifies base material [18]

Fig. 3 Estimated and modelled residual stress distributions in the x-direction for **a** AW condition and **b** HFMI condition weld toe centreline and ±3.5 mm distance from the centreline, where zero normalized depth equals weld toe surface (see Fig. 3 for x- and y-directions) [18]
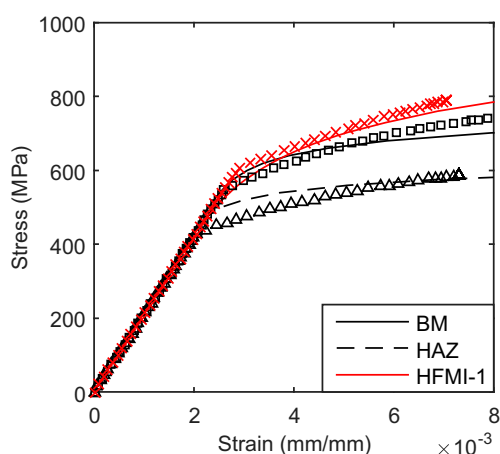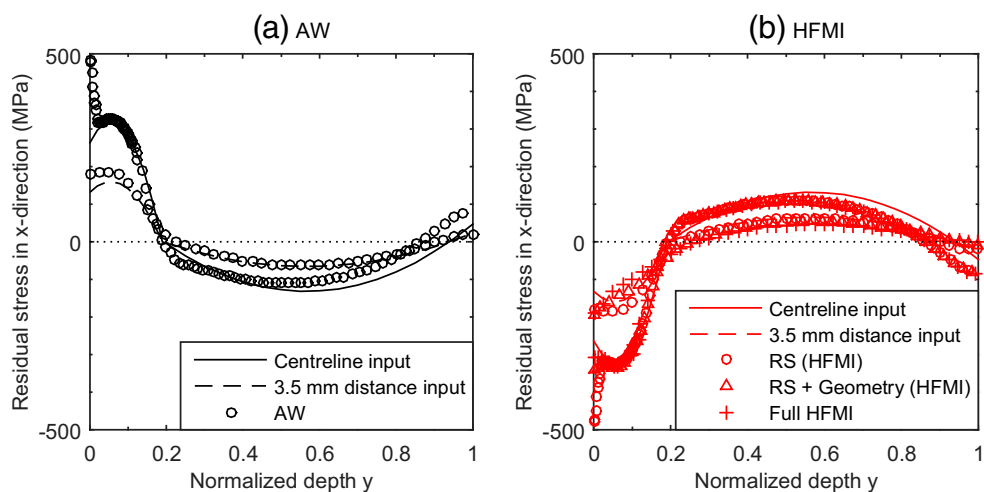

Fig. 4 Comparison of experimental and modelled half-life cyclic stress–strain curves, where the *lines* signify behaviour estimated from experiments [15] and the *symbols* indicate model response [18]

modelled and experimentally estimated half-life stress–strain curves and stress evolution is given in Fig. 4. The experimental stress–strain curves represent average experimentally observed behaviour, whereas the modelled behaviour corresponds to single specimen behaviour. The differences between these two

reflect therefore the observed variation in the test series. For strains above 1 %, further hardening was limited as a conservative assumption due to lack of experimental data. A detailed description of the residual stress distributions and local material properties is given in Mikkola et al. [18].

For AW, weld toe radius of $r = 0.25$ mm was assumed. HFMI-groove was described using average radius r of 3.3 mm, depth of 0.2 mm, and width of 3.8 mm based on measurements by Yıldırım and Marquis [16]. Linear plane strain elements were used as transverse contraction at the weld toe was constrained due to high stress concentration. Finite strain theory was applied to allow large displacements and material nonlinearity. The minimum element size was 0.025 mm in the AW toe region and 0.1 mm in the HFMI-groove region. Global element size was 1 mm. An example of applied mesh corresponding to Fig. 2a is shown in Fig. 5b. Note, however, that in Fig. 5b, the weld toe radius is 1 mm instead of 0.25 mm assumed in the elastic-plastic simulations.

The applied loading histories represented CA loading with different stress ratios and the effects of peak stresses during VA loading. CA loading was applied at two nominal stress range levels experimentally observed to result in
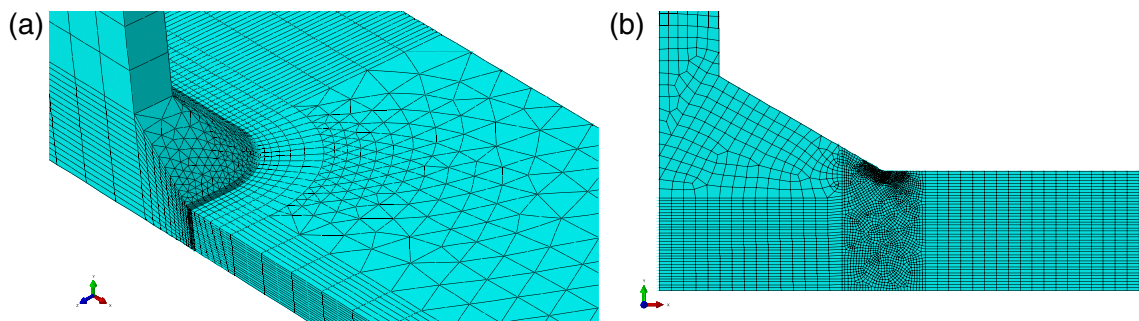

Fig. 5 Examples of applied meshes in the notch stress FE-analyses for **a** a specimen from project FATWELDHSS [10] and **b** simulated AW condition from [18]

Table 3 VA loading data for HFMI-treated longitudinal attachments

Ref.	Steel grade	f_y (MPa)	Method	t (mm)	k	R	S_{max}/f_y
[15]	S700	690[a]	HFMI	8	10	−1	0.54, 0.70
[16]	S700	700[a]	UIT	8	1	−1	0.46
[16]	S960	969[b]	UIT/UP	6	2	−1	0.59, 0.76
[10]	S700MC	700[a]	UIT	5, 10	11	−1	0.55, 0.60, 0.65
[10]	S690QL	690[a]	UIT	10	5	−1	0.50, 0.60, 0.65
[10]	S960MC	960[a]	UIT	5	5	−1	0.45, 0.50, 0.55, 0.60
[10]	S960QL	960[a]	UIT	10	6	−1	0.55, 0.60, 0.65

[a] f_y is a nominal value

[b] f_y is a measured value

approximately 4×10^5 and 2×10^6 cycles to failure in HFMI-treated transverse non-load-carrying attachments [12]. For $R = -1$ and 0, this corresponded to nominal stress ranges of 425 and 300 MPa, whereas for $R = 0.5$, this corresponded to nominal stress ranges of 300 and 250 MPa for HFMI-treated joints. The loading histories representing peak stress effects during VA loading consisted of one peak stress cycle or reversal and 20 CA loading cycles. The applied stress ratio was constant at $R = -1$, and the CA loading stress range was $\Delta S = 300$ MPa in each case. The applied peak stresses were chosen to represent different critical cases in relation to nominal yield strength f_y:

– $0.45f_y$ corresponds to the proposed maximum stress amplitude limit for $R = -1$, see Eq. (2)
– $0.6f_y$ is close to peak stresses applied during VA loading by Yıldırım and Marquis [15].
– $0.8f_y$ corresponds to the maximum stress limit for hammer and needle peened joints [5].

3.2 Notch stress analysis of HFMI-treated joints subjected to VA loading

The problem with expressing the allowable maximum stress range in terms of nominal stress, as in Eq. (2), is that the nominal stress approach does not take into account the effects of joint type and dimensions on the local stress concentration. As the local stress concentration is critical with respect to yielding, estimating residual stress relaxation based on nominal stresses is not straightforward. Therefore, effective notch stress approach [23] was used to correlate the simulated residual stress relaxation and

fatigue damage with experimentally observed fatigue behaviour in HFMI-treated joints. The effective notch stress at the weld toe was determined with elastic FE analysis assuming a 1 mm reference radius for both AW and HFMI-improved joints [3]. The notch stress factor was defined as $K_n = S_n/S$, where the notch stress S_n corresponds to the maximum principal stress at the weld toe and S is nominal stress.

Table 3 summarizes the studied fatigue data on HFMI-improved joints [10, 15, 16] subjected to high peak stresses during VA loading. The data consist of axially loaded longitudinal attachments with plate thicknesses ranging from 5 to 10 mm and yield strengths of approximately 700 and 960 MPa. The total number of data points is $k = 39$. Constant stress ratio of $R = -1$ was applied in each case. As shown by Table 3 and Eq. (2), the applied peak stresses exceeded the allowable stress range limit ΔS_{max} in all cases except one. Damage sum of $D = 1.0$ was used to compute the equivalent stress ΔS_{eq} using Eq. (1), as this is considered a conservative assumption when evaluating test data. Further details of the applied spectra are given in Table 4 and can be found in the references [10, 15, 16]. For comparison, Table 5 summarizes corresponding AW data. Note that in Yıldırım and Marquis [16], the AW joints were subjected to CA loading instead of

Table 4 Details of the applied VA loading spectra

Ref.	Spectrum type	Spectrum length N	R	ΔS_{min}
[15]	Random log-linear	250,000	−1	$0.16\Delta S_{max}$
[16]	Random log-linear/Gaussian	100,000	−1	$0.25\Delta S_{max}$
[10]	Random log-linear	100,000	−1	$0.15\Delta S_{max}$

Table 5 Fatigue data for AW longitudinal attachments corresponding to test series in Table 3

Ref.	Steel grade	f_y (MPa)	t (mm)	k	R	Scenario	S_{max}/f_y
[15]	S700	690[a]	8	5	−1	VA	0.36, 0.54, 0.70
[16]	S700	700[a]	8	9	−1	CA	< 0.45
[16]	S960	969[b]	6	-	-	-	-
[10]	S700MC	700[a]	5, 10	17	−1	VA	0.40, 0.45, 0.50, 0.55
[10]	S690QL	690[a]	10	−	-	-	-
[10]	S960MC	960[a]	5	12	-1	VA	0.40, 0.45, 0.50, 0.55
[10]	S960QL	960[a]	10	-	-	-	-

[a] f_y is a nominal value

[b] f_y is a measured value

VA loading. In the references [10, 15], a similar VA loading spectrum was applied for both AW- and HFMI-treated joints.

The longitudinal attachments used in references [10, 15, 16] were modelled in 3D according to given global dimensions. Due to varying dimensions, the K_t values will be different even though the joint type was the same in all cases. One eighth of the attachment was modelled in each case, as all joints were symmetrical. Actual weld geometry and resulting notch stress concentration value K_n were reported only in Yıldırım and Marquis [15]. In the other cases, a weld angle of 45° was used as recommended in Hobbacher [20]. Weld leg length of 8 mm was assumed for simplicity. All welds in Vanrostenberghe et al. and Yıldırım and Marquis [10, 15] were full penetration welds. In Yıldırım and Marquis [16], this was not always the case. However, as most data were from full penetration welds and the focus was on weld toe stress concentration, weld roots were not modelled. The error resulting from the different modelling assumptions was considered small enough not to affect the conclusions. Reference radius of 1 mm was used in all cases as recommended in Marquis [3]. Elastic modulus of 210 GPa and Poisson's ratio of 0.3 were used to describe the elastic material response. Second-order solid elements were used in the analysis. Maximum and minimum element sizes were $t/4$ and $r/10$, respectively, with t indicating plate thickness and r notch radius. An example of the applied mesh is given in Fig. 5a. The previously simulated transverse attachment [18] with a reference radius of 1 mm was analysed in 2D due to symmetry. The used element sizes were smaller than $t/4$ and $r/10$, see Sect. 3.1 and Fig. 5b.

4 Results

4.1 Simulated residual stress relaxation

The simulations focused on the response at the assumed crack initiation location, i.e. the weld notch root.

Therefore, the presented stress–strain curves give maximum principal stress values at x = 0 and y = 0.05 mm—see Fig. 2 for definition of x- and y-axes. For $R = -1$ and 0, the response in the full HFMI condition was approximately elastic under the applied nominal stress ranges, and no residual stress relaxation was observed. For $R = 0.5$, compressive residual stresses relaxed fully for all joint conditions, as shown by Fig. 6. The shift from point A to point B indicates the level of residual stress relaxation at the weld notch root. However, the results indicated that improved notch geometry and strain hardening had some beneficial effect, as they decreased the stress and strain ranges and the level of yielding with respect to AW and RS (HFMI) conditions, as shown by Fig. 6b, c compared to Fig. 6a. Similarly, benefit from geometry improvement and strain hardening was observed for $R = -1$ and 0.

Figure 7 shows the simulated stress–strain response for AW and full HFMI conditions under different peak stress magnitudes. Letters A and F give the start and end locations, whereas the letters from B to E indicate the succession of peaks and valleys in the applied loading history. All applied peak stress magnitudes resulted in residual stress relaxation in the full HFMI condition. For $S_{max/min} = \pm 0.45 f_y$ in Fig. 7a, residual stress relaxation was limited, and the local mean stress at the weld toe remained compressive. $S_{max/min} = \pm 0.6 f_y$ resulted in full residual stress relaxation, as shown by Fig. 7b, whereas $S_{max/min} = \pm 0.8 f_y$ resulted in tensile mean stress, as shown by Fig. 7c. When compared to a similar load AW joint condition in Fig. 7d, it was seen that the AW local mean stress was higher than the full HFMI local mean stress even after residual stress relaxation. In addition, the stress and strain ranges for the simulated AW case were higher than for the corresponding full HFMI case. This was due to higher stress concentration and lower local strength in the simulated AW condition.

In addition to the peak stress simulations shown in Fig. 7, the peak stress location and type in the loading history were varied [18]. These simulations showed that with respect to
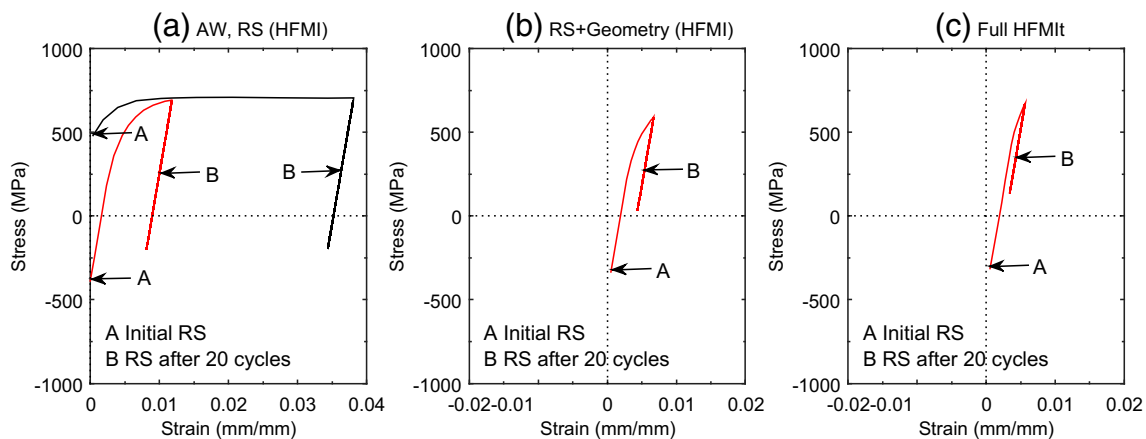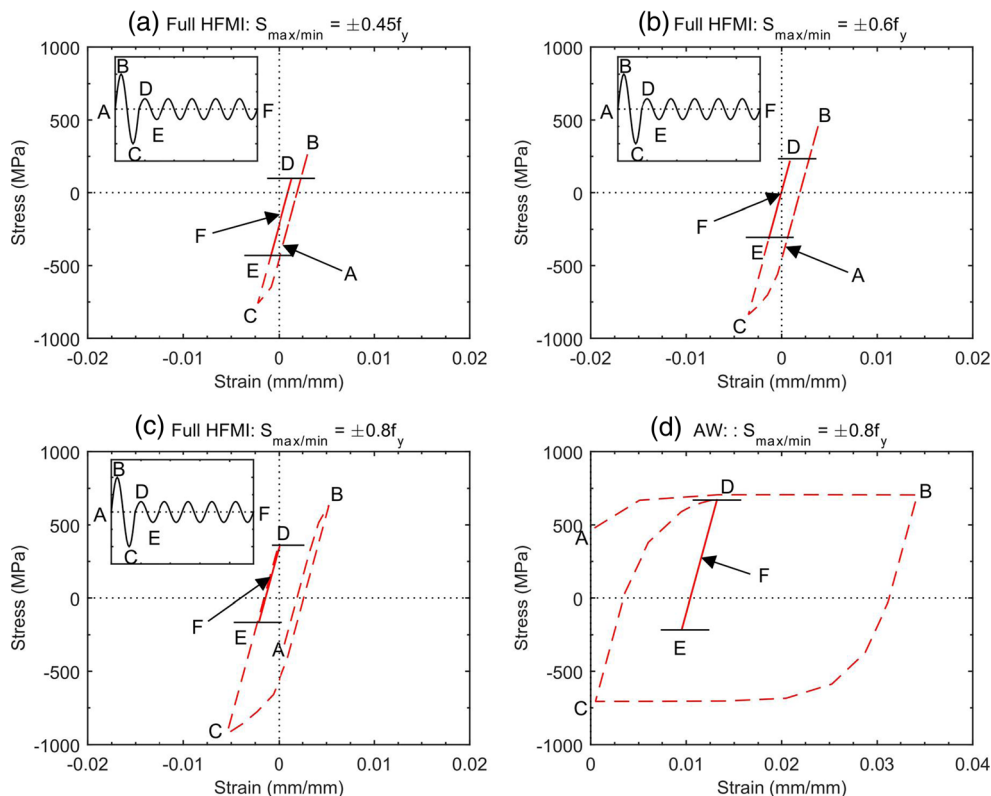

Fig. 6 Simulated local stress–strain response for **a** AW and RS (HFMI), **b** RS + geometry (HFMI) and **c** full HFMI under CA loading when $R = 0.5$ and $\Delta S = 300$ MPa modified from [18]

Fig. 7 Simulated local stress–strain response for **a**–**c** full HFMI and **d** AW conditions. The CA loading is with $R = -1$ and $\Delta S = 300$ MPa [18]

residual stress relaxation of compressive residual stresses, the compressive reversal was critical, whereas the tensile reversal had little effect on local mean stress. In addition, a second peak stress cycle increased the local mean stress further, but the level of residual stress relaxation was low relative to the first peak stress cycle.

Smith-Watson-Topper parameter [24] $P_{SWT} = (\sigma_{max}\Delta\varepsilon/2)^{0.5}$, where $\Delta\varepsilon$ is the strain range and σ_{max} is the maximum

stress in the first closed hysteresis loop, was used to estimate relative fatigue damage. Figure 8 shows relative fatigue damage estimated from the stress–strain response in Fig. 6 and Fig. 7. For comparison, estimated fatigue damage in $R = -1$ CA loading simulations [18] is presented in Fig. 8b. Figure 8a shows that for $R = 0.5$, the benefit from compressive residual stresses is lost. The main benefit comes from geometry improvement. The influence of strain hardening is not as clear
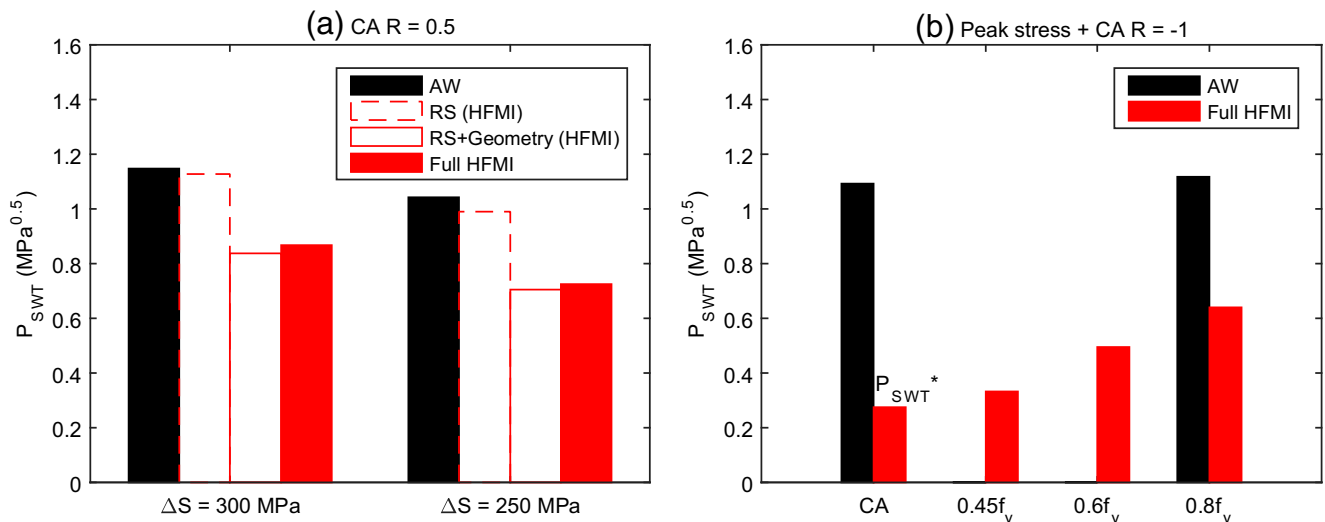

Fig. 8 Estimated fatigue damage parameter values for **a** $R = 0.5$ CA loading and **b** different peak stress magnitudes for different joint conditions based on stress–strain response in Fig. 6 and Fig. 7, where the CA loading in **b** is with $\Delta S = 300$ MPa for both CA loading and peak

stress simulations and $P_{SWT}{}^* = P_{SWT} \times (300 \text{ MPa}/425 \text{ MPa})$ is a modified value based on the P_{SWT} value for $\Delta S = 425$ MPa, modified from Mikkola et al. [18]

Table 6 Estimated notch stress factors for longitudinal attachments subjected to VA loading available in literature modified from [19]

Reference	t (mm)	K_n	$K_{n,min}$
Simulations [18]	20	2.24	2.10
Yıldırım and Marquis [15]	8	2.36[a]	2.10
Marquis and Björk [16]	6	2.81	2.10
Marquis and Björk [16]	8	3.13	2.70
FATWELDHSS [10]	5	2.92	2.10
FATWELDHSS [10]	10	3.36	2.70

[a] Value from Yıldırım and Marquis [25] based on actual weld angle and leg length

due to higher local yield strength of the full HFMI condition, which increased the local maximum stress compared to RS + geometry (HFMI). However, benefit from strain hardening is expected based on higher fatigue resistance of the HFMI material condition when compared to HAZ material condition, as discussed in Mikkola et al. [18]. Figure 8b shows that fatigue damage increases with increasing peak stress magnitude for full HFMI. Nevertheless, benefit with respect to the AW state in terms of the calculated fatigue damage is observed even for the highest peak stress magnitude.

4.2 Notch stresses

The estimated notch stress factors for the VA data sets are given in Table 6. All calculated values were above recommended minimum notch stress factors $K_{n,min}$ [25]. The simulated transverse attachment had the lowest stress concentration factor, which is to be expected since this type is typically less severe than the longitudinal attachment used in the experiments. For comparing the peak stresses in the

experiments and simulations, the nominal maximum stresses were multiplied by the estimated notch stress factors K_n. Figure 9 shows the relationship of maximum nominal stress S_{max} divided by f_y and maximum effective notch stress $S_{n,max}$ divided by f_y for the experimental VA loading cases and the simulations. All test data except one correspond to fatigue failure as indicated in Fig. 9. Even though the simulations had the highest maximum nominal stress with respect to yield strength S_{max}/f_y, the maximum notch stresses with respect to yield strength $S_{n,max}/f_y$ were generally higher in the fatigue tests. This indicates that the applied peak stresses in the VA fatigue tests, where $S_{min} = -S_{max}$, were most likely large enough to result in significant residual stress relaxation, as the simulations indicate full residual stress relaxation for $S_{max}/f_y = 0.6$. According to the current proposal [3], benefit from HFMI treatment could not be claimed for any of these cases, as indicated in Fig. 9.

4.3 Fatigue life comparison

Figures 10 and 11 show the analysed HFMI VA fatigue data in terms of equivalent effective notch stress range $K_n \cdot \Delta S_{eq}$. Only toe failures and run-outs were considered. For comparison, available AW data with corresponding steel grade and welding process are shown. The characteristic curves are FAT 225 for AW joints according to Fricke [23] and FAT 400 and 500 for HFMI-treated welded joints as proposed in Marquis et al. [3], see Fig. 1. The HFMI data are categorized based on the applied nominal peak stress magnitudes. The figures show that all HFMI data points are close to or above the proposed FAT 400 and 500 curves. Clear benefit from HFMI treatment in comparison to AW FAT 225 curve is observed for all cases, except for the

Fig. 9 Relationship of estimated maximum notch and nominal stresses in comparison to yield strength in VA $R = -1$ data and simulations [18], where FATWELDHSS indicates data from Vanrostenberghe et al. [10] and $S_{max}/f_y = 0.6$ corresponds to full residual stress relaxation in the simulations [19]
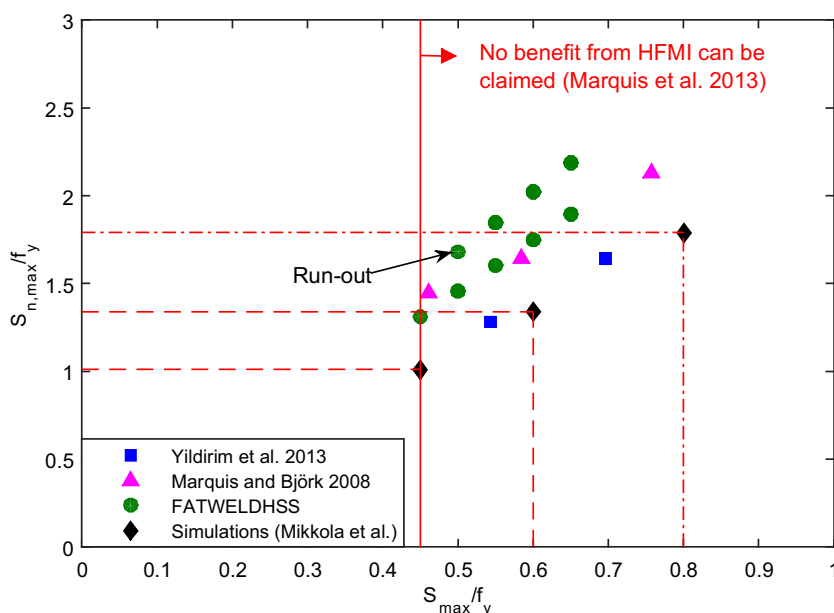
Fig. 10 Fatigue data of HFMI-treated joints subjected to VA $R = -1$ loading in terms of equivalent notch stress from **a** FATWELDHSS project [10] and **b** [15, 16] modified from Mikkola [19]
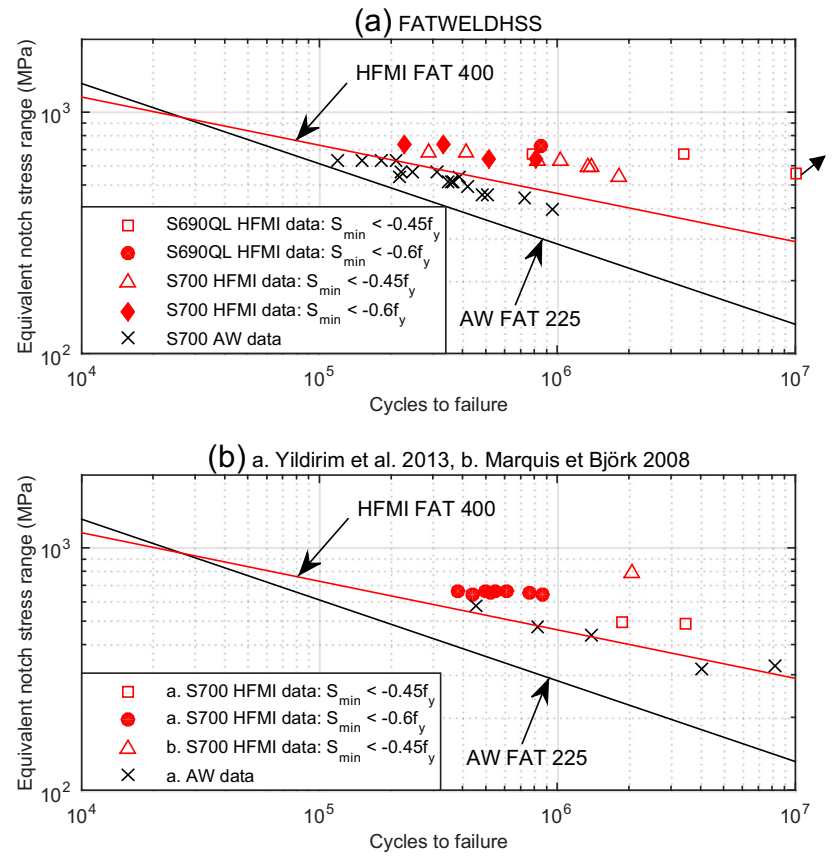

Fig. 11 Fatigue data of HFMI-treated joints subjected to VA $R = -1$ loading in terms of equivalent notch stress from **a** [16] and **b** FATWELDHSS project [10] modified from Mikkola [19]
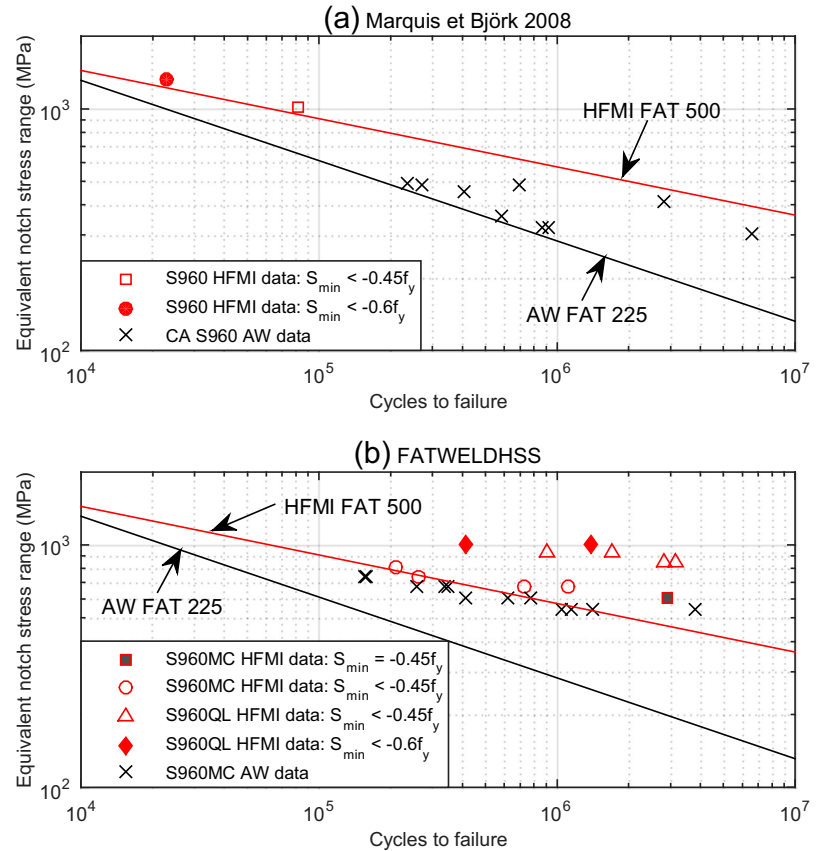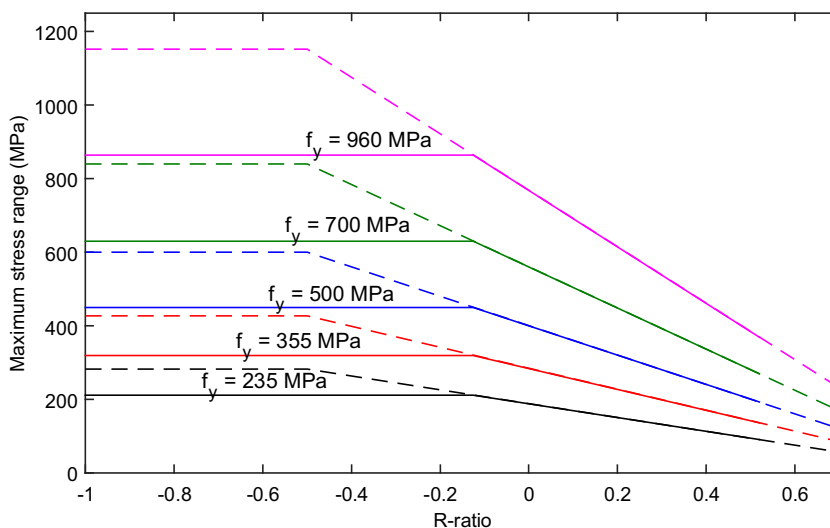
Fig. 12 Applied maximum nominal stress range ΔS_{max} limits. *Solid lines* represent proposed limits according to Eq. (2) and *dashed lines* represent suggested update according to Eq. (3) modified from Mikkola [19]

two data points in Fig. 11a, where the increase in fatigue strength with respect to AW curve is limited due to high equivalent stress range. Comparison of the AW data to the AW and HFMI curves indicates high welding quality. As a result, the increase in fatigue strength from AW state to HFMI-treated state in Figs. 11 and 12 is not as large as the increase in fatigue class from AW FAT 225 to HFMI FAT 400 or 500. This is because the AW FAT is based on a large range of welding qualities. However, the estimated characteristic stress ranges ΔS_c indicate benefit from HFMI treatment in all cases, where comparison is possible (see Table 7). Table 8 gives the estimated percent fatigue strength improvement at 2×10^6 cycles where applicable.

Figures 11 and 12 together with Table 7 clearly show that the proposed fatigue classes FAT 400 for $550 < f_y \leq 750$ MPa and FAT 500 for $950 < f_y$ fitted the HFMI data, even though significant residual stress relaxation has been observed in Fig. 10b tests [15] and has likely occurred in all cases based on Fig. 9. For an individual HFMI data set, the level of fatigue strength improvement with respect to AW condition tends to decrease with increasing peak stress. However, relatively large differences in fatigue strength depending on steel type are observed independent of the applied peak stress. This is also indicated by Fig. 10: there is no clear relation between level of improvement and applied peak stress level. However, due to limited number of data available, there is considerable uncertainty with respect to the effects of peak stresses—and VA loading in general—on fatigue strength improvement. Nevertheless, the notch stress analysis gives confidence that a higher maximum stress range limit of at least $1.2f_y$ for $R = -1$, corresponding to $S_{max/min} = \pm 0.6f_y$ when $R = -1$, could be applied to allow further benefit from HFMI treatment under VA loading.

5 Discussion

Residual stress relaxation in a transverse attachment was simulated to investigate allowable stresses in HFMI-improved welded joints. For $S_{min} = -0.6f_y$, the simulations showed full

Table 7 AW and HFMI FAT values together with estimated characteristic stress ranges at 2×10^6 cycles with 95 % survival probability using the effective notch stress approach, where fixed slope signifies fixed $m = 5$ for HFMI-treated joints and $m = 3$ for AW joints

Ref.	Steel grade	HFMI FAT	AW ΔS_C (MPa)		HFMI ΔS_C (MPa)		Figure
			Fixed slope $m = 3$	Free slope	Fixed slope $m = 5$	Free slope	
[15]	S700	400	316	347 ($m = 4.4$)	454	459 ($m = 5.2$)	8b
[16]	S700	400	207	220 ($m = 3.6$)	a	a	8b
[16]	S960	500	a	a	a	a	9a
[10]	S700MC	400	263	302 ($m = 3.8$)	452	499 ($m = 7.1$)	8a
[10]	S690QL	400	a	a	416	441 ($m = 8.5$)	8a
[10]	S960MC	500	311	451 ($m = 7.3$)	431	547 ($m = 9.5$)	9b
[10]	S960QL	500	a	a)	696	739 ($m = 8.1$)	9b

[a] Not available due to low number of data or no data

AW FAT is 225 in all cases

Table 8 Estimated improvement in mean fatigue strength at 2×10^6 cycles. S_{max}/f_y and $S_{n,max}/f_y$ correspond to peak stresses applied in tests on HFMI-treated joints

	Steel grade	S_{max}/f_y	$S_{n,max}/f_y$	Fixed slope ($m = 3 \rightarrow 5$)	Free slope
[15]	S700MC	0.54–0.70	1.28–1.64	28 %	27% ($m = 4.4 \rightarrow 5.2$)
[16]	S700	0.46	1.45	a	a
[16]	S960	0.59–0.76	1.64–2.12	a	a
[10]	S700MC	0.55–0.65	1.60–2.19	80 %	69% ($m = 3.8 \rightarrow 7.1$)
[10]	S690QL	0.50–0.65	1.68–2.19	a	a
[10]	S960MC	0.45–0.60	1.31–1.75	38 %	19% ($m = 7.3 \rightarrow 9.5$)
[10]	S960QL	0.55–0.65	1.85–2.19	a	a

[a] Comparison not possible due to lack of corresponding AW data

residual stress relaxation in the full HFMI condition, whereas for $S_{min} = -0.45f_y$, the level of residual stress relaxation was moderate. Residual stress measurements have indicated similar behaviour. For one of the investigated VA loaded specimens (see Fig. 10b), significant residual stress relaxation under VA loading has been observed [15]. The applied nominal peak stresses were $0.54f_y$ and $0.7f_y$, as shown by Table 3. In addition, Khurshid et al. [26] have measured moderate residual stress relaxation for a nominal peak stress magnitude of approximately $0.42f_y$.

The fatigue damage calculations indicated an increase in relative fatigue damage with increasing peak stress magnitude. However, benefit with respect to the simulated AW condition remained even for the highest applied peak stress of $0.8f_y$. The CA loading simulations together with available material test data [27] indicated this to be due to geometry improvement and strain hardening. The estimated benefit from HFMI under peak stresses is in line with experimental observations under VA loading, as shown in Figs. 10 and 11, where all data is above the proposed S–N curves for $R \leq 0.15$. Nevertheless, the influence of residual stress relaxation shows in the fact that the fatigue data is close to the proposed S–N curves corresponding to stress ratios $R \leq 0.15$. With no residual stress relaxation, a further improvement of approximately 38 % would be expected when decreasing the applied stress ratio from $R = 0.1$ to $R = -1$ [3]. The residual stress relaxation simulations and relative fatigue damage analysis in Mikkola et al. [18] indicated a similar level of improvement from $R = 0$ to $R = -1$ under CA loading.

Based on the simulations and available experimental results, it is proposed that peak stresses of at least $S_{min} = -0.6f_y$ could be allowed. The reasoning is that with this compressive peak stress magnitude, both the fatigue test results in Figs. 10 and 11 and the estimated relative fatigue damage indicate clear benefit from HFMI with respect to AW condition. Residual stress measurements [15] and the simulated stress–strain response indicated that $S_{min} = -0.6f_y$ results in close to zero residual stresses. This can still be regarded as improvement with respect to

having tensile residual stresses that are typical in AW joints. For higher peak stresses, the benefit is expected to reduce, as the difference in residual stress state for AW and HFMI-treated welded joints decreases with increasing relaxation of the AW tensile residual stresses. Therefore, $S_{min} = -0.6f_y$ resulting in close to zero residual stresses could be considered an appropriate limit.

The current maximum allowable stress investigation is based on experimental results and simulations under $R = -1$ loading, where the compressive reversal is considered to be the damaging one based on simulation results [18]. With respect to residual stress relaxation, it is expected that higher stresses could be allowed for $R > -1$ based on the lower absolute magnitude of compressive peak stress for these stress ratios. However, due to lack of experimental data and numerical results, a more conservative approach is recommended as shown in Fig. 12. In Fig. 12, the proposed limit of $0.8f_y(1-R)$ is extended to meet the proposed limit of $\Delta S_{max} = 1.2f_y$ or $S_{min} = -0.6f_y$ for $R = -1$. This corresponds to

$$\begin{cases} \Delta S_{max} \leq 0.8f_y(1-R), \text{ for } -0.5 \leq R \leq 0.7 \\ \Delta S_{max} \leq 1.2f_y, \text{ for } -1 \leq R < -0.5 \end{cases}. \tag{3}$$

Note that in Eq. (3) and Fig. 12, the allowable maximum stress ratio is increased from $R = 0.52$ to $R = 0.7$ according to the proposal in Mikkola et al. [7].

Uncertainty with respect to the proposed limits in Eq. (3) rises mainly due to limited number of VA loading data and the fact that the applied spectrums were similar with a constant stress ratio of $R = -1$. In addition, as shown by Table 8, there was no clear link between the applied peak stress magnitudes and the observed improvement from the AW state. This might be due to differences in the original welding quality. However, Figs. 11b and 9 show that in the FATWELDHSS tests [10], there is also a clear difference in fatigue strength between the two different steel grades. Another issue to be considered is fatigue improvement under fluctuating mean stress. From residual stress relaxation point of view, it is expected that

relaxation will occur during one critical cycle due to either high mean stress or large compressive stress. As stated in Mikkola [6], Eqs. (2) and (3) fit available high stress ratio data reasonably well without being overly conservative.

6 Conclusions

Allowable maximum stresses in HFMI-treated joints were investigated by analysing available VA fatigue data and simulating residual stress relaxation in a transverse attachment. Residual stress relaxation in the experiments was then estimated by correlating the applied peak stresses in the experiments with the simulated residual stress relaxation behaviour using effective notch stress analysis. Statistical analysis was performed to estimate the fatigue strength improvement after residual stress relaxation in the experiments. Based on the simulation results and notch stress analysis, $\Delta S_{max} = 1.2 f_y$, corresponding to $S_{min} = -0.6 f_y$ when $R = -1$, was proposed as a maximum stress limit for $R < -0.5$. In addition, the maximum allowable stress ratio was proposed to be increased from $R = 0.52$ to $R = 0.7$.

Further experimental and numerical work is required to confirm the applicability of the suggested stress ratio and maximum stress range limits. In particular, in situ residual stress measurements together with fatigue testing are proposed to determine the effect of VA loading on residual stress relaxation and the resulting fatigue improvement. It is expected that a single large enough peak stress is responsible for residual stress relaxation and that further peak stresses simply increase the equivalent stress range of the spectrum. Finally, simulations with a wider range of VA loading histories and with varying mean stress are proposed for verifying residual stress behaviour under service loading conditions.

References

1. Weich I (2008) Fatigue behaviour of mechanical post weld treated welds depending on the edge layer condition (Ermüdungsverhalten mechanisch nachbehandelter Schweißverbindungen in Abhängigkeit des Randschichtzustands) [Doctoral Thesis]. Technischen Universität Carolo-Wilhelmina
2. Yıldırım HC, Marquis GB (2012) Fatigue strength improvement factors for high strength steel welded joints treated by high frequency mechanical impact. Int J Fatigue 44:168–176
3. Marquis GB, Mikkola E, Yıldırım HC, Barsoum Z (2013) Fatigue strength improvement of steel structures by high-frequency mechanical impact: proposed fatigue assessment guidelines. Welding in the World 57:803–822
4. Farajian-Sohi M, Nitschke-Pagel T, Dilger K (2010) Residual stress relaxation of quasi-statically and cyclically-loaded steel welds. Welding in the World 54:49–60
5. Haagensen PJ, Maddox SJ (2013) IIW recommendations on post weld improvement of steel and aluminium structures. Series in Welding and Other Joining Technologies No. 79. Woodhead Publishing Ltd., Cambridge
6. Mikkola E, Doré MJ, Marquis GB, Khurshid M (2015) Fatigue assessment of high-frequency mechanical impact (HFMI)-treated welded joints subjected to high mean stresses and spectrum loading. Fatigue & Fracture of Engineering Materials & Structures 38:1167–1180
7. Mikkola E, Doré MJ, Khurshid M (2013) Fatigue strength of HFMI treated structures under high R-ratio and variable amplitude loading. Procedia Engineering 66:161–170. doi:10.1016/j.proeng.2013.12.071
8. Maddox SJ, Doré MJ, Smith SD (2011) A case study of the use of ultrasonic peening for upgrading a welded steel structure. Welding in the World 55:56–67
9. Mori T, Shimanuki H, Tanaka M (2012) Effect of UIT on fatigue strength of web-gusset welded joints considering service condition of steel structures. Welding in the World 56:141–149
10. Vanrostenberghe S, Clarin M, Shin Y, et al. (2015) Improving the fatigue life of high strength steel welded structures by post weld treatments and specific filler material (FATWELDHSS). Grant Agreement RFSR-CT-2010-00032. Luxembourg
11. Deguchi T, Mouri M, Hara J et al (2012) Fatigue strength improvement for ship structures by ultrasonic peening. J Mar Sci Technol 17:360–369
12. Kuhlmann U, Dürr A, Bergmann J, Thurmser R (2006) Fatigue strength improvement for welded high strength steel connections due to the application of post-weld treatment methods (Effizienter Stahlbau aus höherfesten Stählen unter Ermüdungsbeanspruchung). FOSTA Research Association for Steel Applications, Düsseldorf
13. Okawa T, Shimanuki H, Funatsu Y et al (2013) Effect of preload and stress ratio on fatigue strength of welded joints improved by ultrasonic impact treatment. Welding in the World 57:235–241
14. Ummenhofer T, Herion S, Hrabowsky J, et al. (2011) REFRESH – Extension of the fatigue life of existing and new welded steel structures (Lebensdauerverlängerung bestehender und neuer geschweißter Stahlkonstruktionen). FOSTA Research Association for Steel Applications (Forschungsvereinigung Stahlanwendung e. Düsseldorf
15. Yıldırım HC, Marquis GB (2013) A round robin study of high-frequency mechanical impact (HFMI)-treated welded joints subjected to variable amplitude loading. Welding in the World 57:437–447
16. Marquis GB, Björk T (2008) Variable amplitude fatigue strength of improved HSS welds. International Institute of Welding, IIW Document XIII-2224-08, Paris
17. Huo L, Wang D, Zhang Y (2005) Investigation of the fatigue behaviour of the welded joints treated by TIG dressing and ultrasonic peening under variable-amplitude load. Int J Fatigue 27:95–101
18. Mikkola E, Remes H, Marquis G (2017) A finite element study on residual stress stability and fatigue damage in high-frequency mechanical impact (HFMI)-treated welded joint. Int J Fatigue 94:16–29. doi:10.1016/j.ijfatigue.2016.09.009
19. Mikkola E (2016) A study on effectiveness limitations of high-frequency mechanical impact [Doctoral Thesis]. May 27, Aalto University School of Mechanical Engineering, Espoo, Finland.

20. Hobbacher A (2016) Recommendations for Fatigue Design of Welded Joints and Components, 2nd ed. doi: 10.1007/978–3–319-23757-2. Springer, Heidelberg, New York.

21. Niemi E (1997) Random loading behavior of welded components. Proc. of the IIW International Conference on Performance of Dynamically Loaded Welded Structures. SJ Maddox and M. Prager (eds), July 14–15, San Francisco, Welding Research Council, New York.

22. Abaqus User Manual (2014) Version 6.14. http://50.16.225.63/v6.14/index.html

23. Fricke W (2012) IIW recommendations for the fatigue assessment of welded structures by notch stress analysis. Woodhead Publishing Ltd., Cambridge

24. Smith R, Watson P, Topper T (1970) A stress-strain function for the fatigue of metals. J Mater 5:767–778

25. Yıldırım HC, Marquis GB (2014) Notch stress analyses of HFMI-improved welds by using $\rho f = 1$ mm and $\rho f = \rho + 1$ mm approaches. Fatigue & Fracture of Engineering Materials & Structures 37:463–579

26. Khurshid M, Barsoum Z, Marquis GB (2014) Behavior of compressive residual stresses in high strength steel welds induced by high frequency mechanical impact treatment. J Press Vessel Technol 136:041404–1–041404–8

27. Mikkola E, Marquis G, Lehto P et al (2016) Material characterization of high-frequency mechanical impact (HFMI)-treated high-strength steel. Mater Des 89:205–214